

Peer-reviewed Letter

A Simple Model of the Combined Electrical-Optical Interaction in Neural Tissue

Duke AR¹, Chiel HJ^{2,3,4} and Jansen ED^{1,5*}

¹Department of Biomedical Engineering, Vanderbilt University, USA

²Department of Biomedical Engineering, Case Western Reserve University, USA

³Department of Biology, Case Western Reserve University, USA

⁴Department of Neurosciences, Case Western Reserve University, USA

⁵Department of Neurological Surgery, Vanderbilt University, USA

*Corresponding author: Jansen ED, Department of Biomedical Engineering, Vanderbilt University, 5317 Stevenson Center, VU Station B 350079, Nashville, TN 37235-1631, USA

Received: June 05, 2014; Accepted: June 07, 2014; Published: June 09, 2014

Over the last decade there has been increasing enthusiasm for optical methods of probing and controlling excitable tissues, including optogenetics, optical uncaging, and infrared neural stimulation. Each of these methods has respective advantages and disadvantages that make them well suited for different applications. We have focused on the application of pulsed infrared light as a spatially-precise, non-contact, and artifact-free form of neural control [1]. We have shown that the pulsed temperature transients induced by spatially confined infrared pulses are capable of both eliciting and inhibiting action potential propagation [1,2]. We also showed that sub-threshold infrared and electrical stimulation can be combined to evoke a neural response [3,4]. While the complete mechanism of infrared induced activation is yet to be elucidated and a comprehensive model is still lacking, previous studies showed that a thermally-mediated change in electrical capacitance of the plasma membrane plays a key role [5]. Here we offer a plausible, simplified explanation for how infrared-induced temperature transients are applied towards both hybrid electro-optical stimulation and infrared inhibition.

Previous studies indicate that any model of interactions between infrared light and neural tissue must account for the induced temperature rise [5,6]. At its most basic level, this includes accounting for temperature changes in the Hodgkin-Huxley (HH) model of action potential initiation and propagation [7]. The HH model introduced gating variables to express the time and voltage dependence of the ionic conductances in the squid giant axon. The equation for the potassium conductance is:

$$g_K = \bar{g}_K n^4 \quad (1)$$

where \bar{g}_K (conductance/cm²) is a constant and n is the dimensionless gating variable ranging from 0 to 1 that indicates

the portion of molecules in a certain position (e.g. inside of the membrane). Similarly, the sodium conductance is given by:

$$g_{Na} = m^3 h \bar{g}_{Na} \quad (2)$$

where m is the portion of hypothetical activating molecules on the inside of the membrane and h is the proportion of activating molecules on the outside. Each gating variable is time, voltage and temperature dependent, and is modeled by:

$$n = \left[-(\alpha_n + \beta_n) \cdot n + \alpha_n \right] \cdot k \quad (3)$$

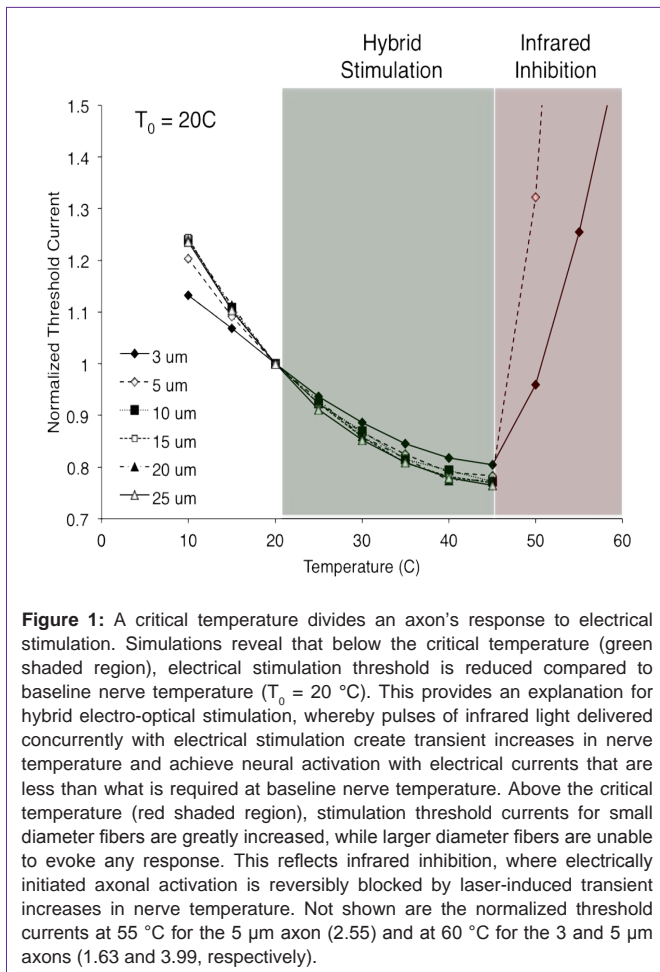
where α_n and β_n are the opening and closing rates of the gates and k is a thermal coefficient [8]. Equation (3) is also used to model the other gating variables (i.e. m and h). Frankenhaeuser and Huxley extended the original HH equations to myelinated fibers, which involved slight variations to equations (1) and (2), as well as the addition of a delayed non-specific ionic current, i_p , and its gating variable p [8,9].

The thermal coefficient, k , in equation (3) determines the acceleration of the opening and closing rates for each gate as the temperature deviates from a predetermined baseline [8]. k is determined by

$$k = Q_{10}^{(T-T_0)/10} \quad (4)$$

Where T is the actual temperature and Q_{10} is a constant used to quantify rate acceleration for a 10 °C increase in temperature. Hodgkin et al. found that a Q_{10} of 3 would allow for comparisons across temperature [10]. However, a Q_{10} of 3 will not simulate an action potential in mammalian axons at 37 °C. Thus, accurate simulations matching empirical results require distinct temperature coefficients for each α and β [8,11]. To model empirical results accurately, the temperature coefficients for the n , h and p rate constants are all close to 3, while the m rate constants are approximately half that. Thus, as the nerve temperature increases, the rates of sodium inactivation (h) and potassium activation (n) overtake the rate of sodium activation (m). This results in an action potential that is either faster and weaker, or completely and reversibly blocked [12,13].

Understanding how this increase in temperature (as induced by a laser pulse) both enhances and inhibits the nerve's response to electrical stimulation requires a closer look at the relationship between nerve temperature and the threshold electrical current for stimulation. Figure 1 shows the results of modeling simulations investigating how electrical stimulation threshold changes with temperature for various nerve fiber diameters. NEURON software (version 7.2) was used to model the myelinated *Xenopus laevis* sciatic nerve and simulate the response to an extracellular electrical point stimulus [11,14]. The temperature of the node of Ranvier directly beneath the electrical stimulus was adjusted independent of all other nodes and internodes to reflect the temperature change resulting from an ideally targeted infrared pulse [11]. Temperature coefficients



were the same as those used by Mou et al. [11]. When the temperature of the node was increased to 45°C (with $T_0 = 20^\circ\text{C}$), the threshold current for an electrically initiated action potential occurring at that node was reduced by up to $\sim 20\%$. Hybrid electro-optical stimulation as we previously demonstrated is likely the result of this temperature increase [3,4,15]. In those studies, the electrical stimulation threshold was first found at baseline temperature (T_0) and then subsequently reduced to 90% of threshold. Providing a concurrent increase in nerve temperature via infrared laser exposure reduces the requisite current for stimulation, thus achieving hybrid activation with a previously sub-threshold electrical stimulus. However, if laser exposure is such that the node temperature surpasses a certain threshold (45°C for these modeling studies), electrically initiated axonal activation will be blocked. Above 45°C , axons $\geq 10\ \mu\text{m}$ in diameter were unable to elicit a propagating action potential at currents many times greater than threshold at T_0 . Axons $\leq 5\ \mu\text{m}$ in diameter were still able to elicit propagating responses, though they required currents that were often much greater than at T_0 . These results are in agreement with those presented by Mou et al. showing that larger diameter fibers (or higher stimulus currents) allowed for lower blocking temperatures [11]. This phenomenon offers an explanation for the inhibitory results we showed previously [2,4]. Thus there appears to be a critical infrared (or otherwise) induced temperature that divides the nerve's response into two regimes: below the critical temperature the electrical

stimulation threshold is reduced to produce hybrid electro-optical stimulation; above the critical temperature the axonal initiation of action potentials is inhibited.

The effect of temperature on the HH gating variables, and their ultimate effects on ionic conductance, provides a plausible explanation for how a laser-induced temperature rise can lead to both hybrid electro-optical stimulation and infrared inhibition. However, interpretation of the simulation results must take into considerations the limitation of the model. This model of a single, myelinated axon only looks at the effect of constant temperature in a single node and does not consider the spatial and temporal evolution of a laser-induced temperature rise in three dimensions. Any laser-induced capacitive currents are also neglected in this model [5]. Shapiro et al. demonstrated that oocytes expressing voltage-gated sodium and potassium channels exhibit a transient capacitive current in response to infrared stimulation and will fire an action potential if the infrared pulse is combined with a just sub-threshold depolarizing electrical stimulus [5]. Rather than two distinct mechanisms, it is more likely that transient capacitive currents and local increases in temperature both contribute to hybrid electro-optical stimulation, as well as infrared inhibition.

While the aforementioned discussion describes a simple and plausible explanation for temperature-induced effects on action potential behavior, it is by no means a complete description of this phenomenon. The next iteration of models and simulations should seek to incorporate these temperature effects with more complex interactions, such as changes in electrical capacitance and light propagation in tissue.

Acknowledgement

This work was made possible by funds from the Department of Defense (HR0011-10-1-0074), the National Institutes of Health (NS-047073) and the National Science Foundation (DMS-1010434).

References

1. Wells J, Kao C, Jansen ED, Konrad P, Mahadevan-Jansen A. Application of infrared light for in vivo neural stimulation. *J Biomed Opt.* 2005; 10: 064003.
2. Duke AR, Jenkins MW, Lu H, McManus JM, Chiel HJ, Jansen ED. Transient and selective suppression of neural activity with infrared light. *Sci Rep.* 2013; 3: 2600.
3. Duke AR, Cayce JM, Malphrus JD, Konrad P, Mahadevan-Jansen A, Jansen ED. Combined optical and electrical stimulation of neural tissue in vivo. *J Biomed Opt.* 2009; 14: 060501.
4. Duke AR, Lu H, Jenkins MW, Chiel HJ, Jansen ED. Spatial and temporal variability in response to hybrid electro-optical stimulation. *J Neural Eng.* 2012; 9: 036003.
5. Shapiro MG, Homma K, Villarreal S, Richter CP, Bezanilla F. Infrared light excites cells by changing their electrical capacitance. *Nat Commun.* 2012; 3: 736.
6. Wells J, Kao C, Konrad P, Milner T, Kim J, Mahadevan-Jansen A, et al. Biophysical mechanisms of transient optical stimulation of peripheral nerve. *Biophys J.* 2007; 93: 2567-2580.
7. Hodgkin AL, Huxley AF. A quantitative description of membrane current and its application to conduction and excitation in nerve. *J Physiol.* 1952; 117: 500-544.
8. Rattay F, Aberham M. Modeling axon membranes for functional electrical stimulation. *IEEE Trans Biomed Eng.* 1993; 40: 1201-1209.

9. Frankenhaeuser B, Huxley AF. The action potential in the myelinated nerve fiber of *Xenopus laevis* as computed on the basis of voltage clamp data. *J Physiol.* 1964; 171: 302-315.
10. Hodgkin AL, Huxley AF, Katz B. Measurement of current-voltage relations in the membrane of the giant axon of *Loligo*. *J Physiol.* 1952; 116: 424-448.
11. Mou Z, Triantis IF, Woods VM, Toumazou C, Nikolic K. A simulation study of the combined thermoelectric extracellular stimulation of the sciatic nerve of the *Xenopus laevis*: the localized transient heat block. *IEEE Trans Biomed Eng.* 2012; 59: 1758-1769.
12. Hodgkin AL, Katz B. The effect of temperature on the electrical activity of the giant axon of the squid. *J Physiol.* 1949; 109: 240-249.
13. Huxley AF. Ion movements during nerve activity. *Ann N Y Acad Sci.* 1959; 81: 221-246.
14. Hines ML, Carnevale NT. *The NEURON Simulation Environment*. Neural Comput. MIT Press 238 Main St., Suite 500, Cambridge, MA 02142-1046 USA, 1997; 9: 1179-1209.
15. Duke AR, Peterson E, Mackanos MA, Atkinson J, Tyler D, Jansen ED. Hybrid electro-optical stimulation of the rat sciatic nerve induces force generation in the plantarflexor muscles. *J Neural Eng.* 2012; 9: 066006.